Smoothly Wavelength-Tunable Picosecond Pulse Generation Using a Harmonically Mode-Locked Fiber Ring Laser

Lingze Duan, *Member, IEEE, Member, OSA*, Mario Dagenais, *Senior Member, IEEE*, and Julius Goldhar

***Abstract*—A simple design of a stable, smoothly wavelength-tunable picosecond pulse generator has been demonstrated using a dispersion-tuned, harmonically mode-locked fiber ring laser with a directly modulated semiconductor optical amplifier (SOA). The SOA functions as both a polarization-insensitive mode locker and a supermode noise suppressor. Near-linearly chirped pulses are generated and compressed to less than 4 ps when the intracavity dispersion is anomalous while 11-ps, near-transform-limited pulses are generated without compression when the dispersion is normal. Smooth wavelength tuning is achieved over more than 11 nm by only tuning the modulation frequency and pulse characteristics are stable over the entire tuning span. A simple numerical model successively simulates the operation principle of the system. The tuning range is determined by both the gain profile and the total intracavity dispersion. The dispersion and the SOA ensure the long-term stability of the system.**

***Index Terms*—Mode-locked lasers, optical fiber dispersion, optical fiber lasers, semiconductor optical amplifiers (SOAs), wavelength tuning.**

I. Introduction

HARMONICALLY mode-locked fiber ring lasers (HMLFRLs) have been widely recognized as promising means to generate high repetition rate, wavelength-tunable picosecond optical pulses [1]–[9]. Conventionally, wavelength tuning in HMLFRLs is realized by changing the center wavelength of a tunable filter inserted in the cavity [2]–[5]. However, the modulation frequency has to be adjusted simultaneously in order to maintain stable pulsing due to intracavity dispersion [5]. This multiparameter tuning process is not only complicated but prone to causing instability as well.

It is desirable in many applications, such as characterization of wavelength-division-multiplexing (WDM) components and subsystems, to have "smoothly" tunable pulse generators, in which the oscillating wavelength can be continuously changed without interrupting the stable pulsing or altering the pulse characteristics. Dispersion tuning is a unique technique that is able to achieve such performance. A dispersion-tuned HMLFRL allows its wavelength being tuned by the repetition frequency or the cavity length while staying mode locked. Single-parameter, smooth wavelength tuning has been successfully realized by several groups [6], [7]. However, little work has been done to address the important issue of supermode noise (SMN) suppression [6] in this type of lasers, which, in part, is because most SMN suppression techniques that have been widely used, such as soliton formation [8] and intracavity filtering [9], impose upon the laser spectral restrictions, which are incompatible with dispersion tuning.

We have previously demonstrated a stable dispersion-tuned HMLFRL by using an intracavity semiconductor optical amplifier (SOA) as a supermode-noise suppressor [10]. The system is able to generate 5.3-ps pulses at 10-GHz repetition rate with a 10-nm wavelength-tuning span. The addition of the SOA improves SMN suppression ratio by 13 dB.

In this paper, we simplify the previous configuration by removing the electrooptic (EO) modulator from the cavity and using the SOA as both a noise suppressor and a mode locker. Our study shows that this compact system outperforms the previous one in various aspects. It produces 3.7-ps pulses at 6 GHz with pulse compression when the intracavity dispersion is anomalous and 11.4-ps near-transform-limited (TL) pulses without pulse compression when the dispersion is normal. A simple numerical model shows good agreement with the experiment.

In the next two sections, we present the experimental and numerical results in anomalous and normal dispersion regimes, respectively. We compare the performances with different configurations in Section IV and draw conclusions in Section V.

II. Anomalous Dispersion Regime

A. Experiment

A schematic of the experimental setup is shown in Fig. 1. The erbium-doped fiber amplifier (EDFA) provided gain to the laser. Its pump power was selected such that the average optical power inside the cavity was kept at a moderate value of 8.5 mW (measured immediately after the EDFA). The SOA (Alcatel 1901) has a typical small signal gain of 25 dB, a typical polarization sensitivity of 0.5 dB, a maximum driving current of 250 mA and a measured transparency current of 24 mA. It was biased slightly above its transparency (25–30 mA) in the experiment. Radio-frequency (RF) power from a synthesized microwave generator was coupled into the SOA via an SMA connector closely attached on the butterfly package. The intracavity group velocity dispersion was provided by 100 m of SMF-28 fiber, which has an anomalous dispersion parameter of 17.7 $\mathrm{ps}/(\mathrm{km}\cdot\mathrm{nm})$ at 1560 nm. A polarization controller (PC) was used to vary the polarization orientation and two

Manuscript received March 28, 2002; revised December 2, 2002.

L. Duan is with the Research Laboratory of Electronics, Massachusetts Institute of Technology (MIT), Cambridge, MA 02139 USA (e-mail: diz@mit.edu).

M. Dagenais and J. Goldhar are with the Department of Electrical and Computer Engineering, University of Maryland, College Park, MD 20742 USA.

Digital Object Identifier 10.1109/JLT.2003.810079

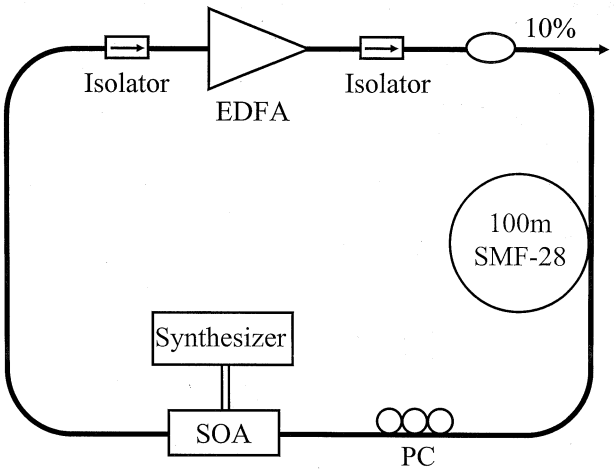

Fig. 1. Experimental setup.

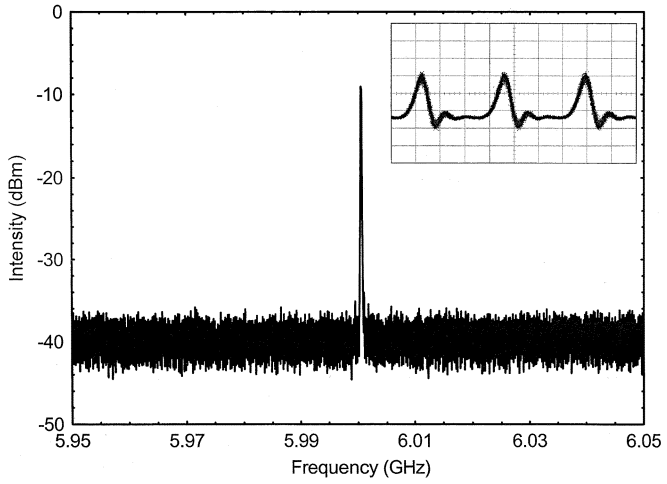

Fig. 2. RF spectrum and sampling oscilloscope trace (inset) of the output pulses with 100-m SMF-28 in the cavity.

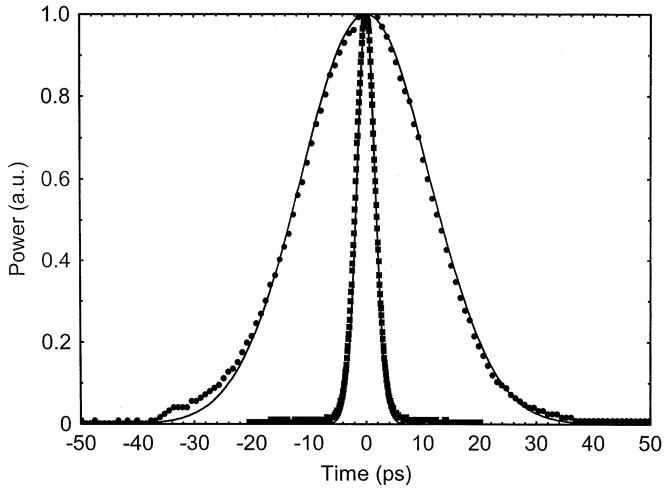

(a)

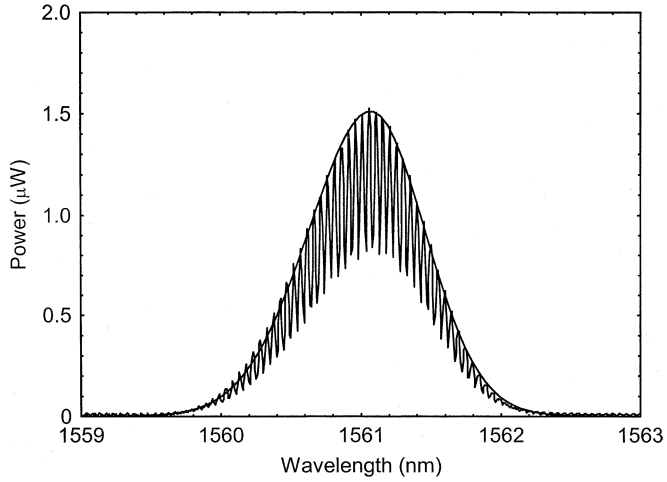

(b)

Fig. 3. Pulse characteristics in time and frequency domains when the intracavity dispersion is anomalous. (a) Autocorrelation traces before and after pulse compression (points are experimental results and curves are numerical results). (b) Spectrum (the envelope curve is numerical result).

Faraday optical isolators ensured a unidirectional cavity. The characteristics of the output pulses were monitored by a sampling oscilloscope (HP 83 480A), an optical spectrum analyzer (Advantest Q8347) and a RF spectrum analyzer (HP 70 001). The pulsewidth was measured by an autocorrelator. Compared to the previous system [10], this configuration is much simpler with the EO modulator and a PC removed.

The experiment was conducted at repetition frequencies around 6 GHz. This value was limited by the RF coupling to the SOA and can be much higher with more sophisticated high-speed packaging [11], [12]. It was observed during the optimization process that the PC had little effect on the pulse characteristics, which indicates that the laser has very weak polarization dependence. This is due to the small polarization sensitivity of the SOA.

Fig. 2 shows the sampling oscilloscope trace (inset) of the output pulses and the output RF spectrum near the modulation frequency. There was no visible amplitude fluctuation on the oscilloscope trace, indicating that the pulse amplitude was well stabilized. Side modes were suppressed below the noise floor on the RF spectrum, giving a 28-dB lower limit of the SMN suppression ratio. A full-width at half-maximum (FWHM) pulsewidth of 25.1 ps and a 3-dB spectral width of 0.943 nm were measured at 1561.1 nm, with the assumption of Sech^2 pulses. With 290 m of dispersion compensating fiber (DCF), the output pulses were compressed down to 3.7 ps, which led to a time-bandwidth product of 0.43. As we point out later, the combination of the direct gain modulation and the anomalous dispersion creates near-linear chirp across the output pulses and, consequently, produces near-TL pulses with linear pulse compression. Fig. 3(a) shows the normalized autocorrelation traces before and after pulse compression and Fig. 3(b) is the optical spectrum, which clearly reveals the locked cavity modes with 6-GHz mode spacing.

Smooth wavelength tuning over 11 nm (1556.9–1568.1 nm) was achieved by varying *only* the modulation frequency within a span of 170 KHz. The spectral peak blue-shifted when the frequency increased, indicting an anomalous total intracavity dispersion, and the oscilloscope trace remained still, indicating stable pulsing throughout the tuning process. The wavelength-frequency relation is linear, as shown in Fig. 4. The pulse characteristics in time and frequency domains were also found stable

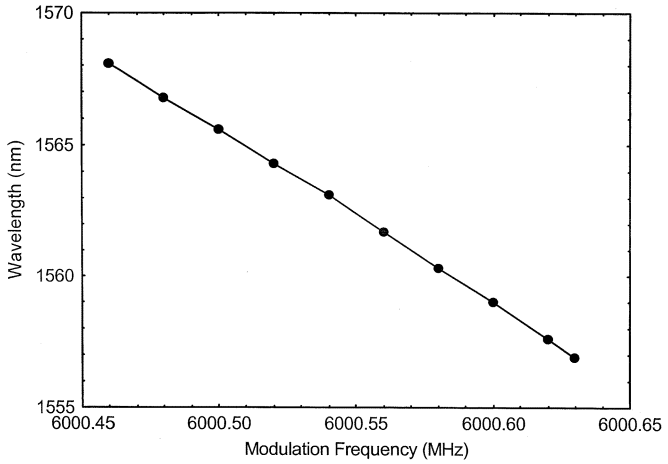

Fig. 4. Oscillating wavelength versus modulation frequency in anomalous dispersion regime (100-m SMF-28 inserted in the cavity).

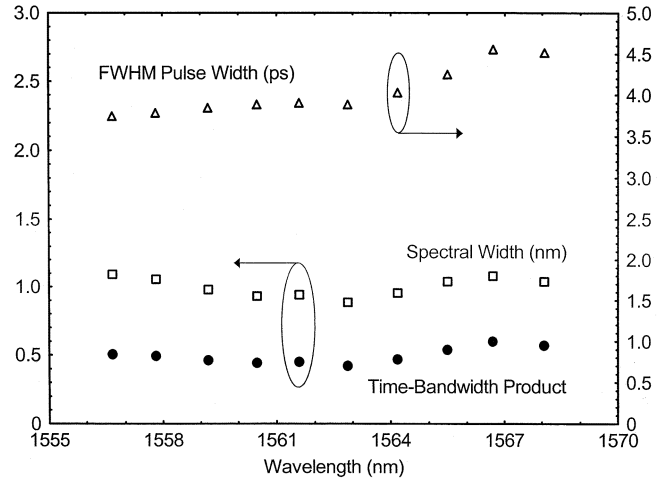

Fig. 5. Measured pulse characteristics with respect to the oscillating wavelength during dispersion tuning with 100-m SMF-28 in the cavity.

during tuning. Fig. 5 shows the compressed pulsewidth (with 290 m DCF), the spectral width and the time-bandwidth product at different wavelengths. The time-bandwidth product ranges from 0.4 to 0.5, indicating near-TL pulses over the entire tuning range.

B. Numerical Simulation

Numerical simulation has been carried out in order to better understand the interaction between the intracavity dispersion and the directly modulated SOA. The algorism is based on the Kuizenga–Siegman approach [13]. The pulse duration is assumed much shorter than the carrier lifetime of the SOA so that the solution of the rate equation can be expressed analytically [14]. Saturation-induced self-phase modulation (SPM) is taken into account through a constant linewidth enhancement factor. External modulation is introduced by sinusoidally varying the small signal gain of the SOA.

The simulation parameters are either experimentally measured values or, in the cases that they are not easily measurable, typical values. The fiber loop is 100-m long, with a total dispersion of 1.7 ps/nm. The modulation frequency is 6 GHz, about 3000th harmonic of the cavity mode. The small signal gain of the SOA and the modulation depth are measured to be approximately 2 dB and 100%, respectively. The linewidth enhancement factor is taken to be 4. The dispersion of the SOA is neglected in the model since it is much smaller than the dispersion of the fiber [15]. The EDFA is assumed to be a completely linear device, which provides a constant gain to balance the loss. The round-trip coupling loss is approximately 12 dB. The DCF for pulse compression has a normal dispersion parameter of $-88\ \mathrm{ps}/(\mathrm{km}\cdot\mathrm{nm})$.

An arbitrarily defined seed pulse is injected into the loop and the resulted pulse solution after each round-trip is calculated until it becomes stable. Fig. 6 shows that stable solutions establish in both time and frequency domains after 400 round-trips. The stable temporal and spectral widths are 28.5 ps and 0.95 nm, respectively. The pulse compression is optimized with 300-m DCF and the minimum pulse duration is 3.8 ps, giving a time-bandwidth product of 0.44. These results are in good agreement with the experiment. Fig. 7 shows the pulse intensity shape before compression and the frequency chirp across the pulse. It is apparent that a proper combination of the directly modulated SOA and the anomalous dispersion leads to near-linearly chirped pulses. This explains the large compression ratio obtained by using the DCF. The autocorrelation functions of the pulses before and after compression are calculated and plotted in Fig. 3(a). The simulated spectrum is plotted in Fig. 3(b). Both results show good agreement with the experiment.

III. Normal Dispersion Regime

In anomalous dispersion regime, external pulse compression is always needed to obtain TL pulses regardless the mode locking element is an EO modulator or an SOA. The few hundred-meter DCF not only reduces the compactness of the system, but also increases the environmentally induced pulse timing variations. It is desirable practically that TL pulses can be generated directly from a mode-locked laser. With the aforementioned numerical model, we find it possible to achieve near-chirp-free pulses when the SOA is directly modulated and the intracavity dispersion is in the normal regime.

A. Experiment

The experimental setup is the same as in Fig. 1, except that the 100 m of SMF-28 is replaced by 25 m of DCF. The SOA and EDFA settings are similar to those in the anomalous-dispersion case. Again, the sampling oscilloscope trace (inset of Fig. 8) of the laser output shows stable pulse amplitude and the RF spectrum (main picture of Fig. 8) at the modulation frequency shows that the side modes are well suppressed. The SMN suppression ratio is more than 29 dB. 11.4-ps pulses are generated at 6 GHz with a time-bandwidth product of 0.35 (Sech^2 pulse shape assumed). It should be stressed that such a small time-bandwidth product is obtained without external pulse compression. The autocorrelation trace and the spectrum of the output pulses are shown in Fig. 9. The well-resolved optical modes in the spectrum indicate stable and phase coherent output. More than 12 nm of wavelength tuning has been achieved (1555.7–1568.1 nm), as shown in Fig. 10. The wavelength-frequency relation is linear but the slope is reverse to it in the anomalous regime. The pulse

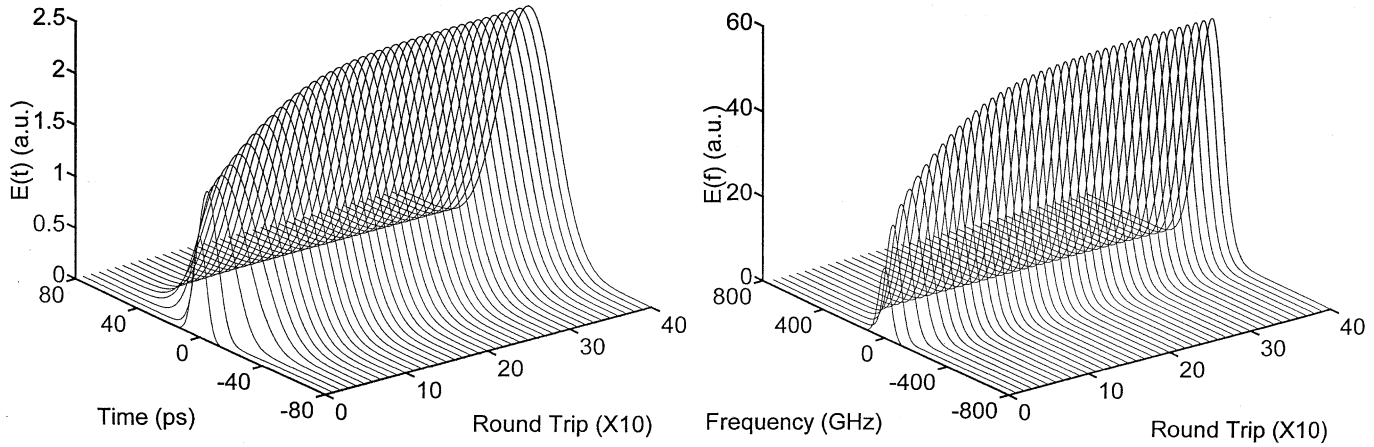

Fig. 6. Stable solutions establish from an initial pulse in both time (left) and spectral (right) domains after 400 round-trips.

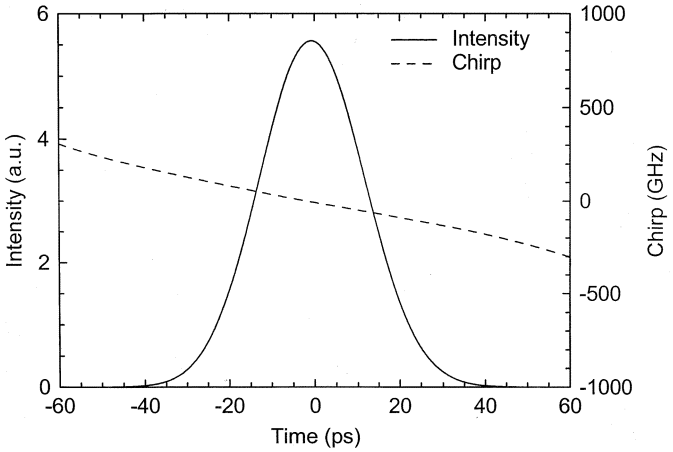

Fig. 7. Simulation result of the time dependence of the pulse intensity (before compression) and the frequency chirp.

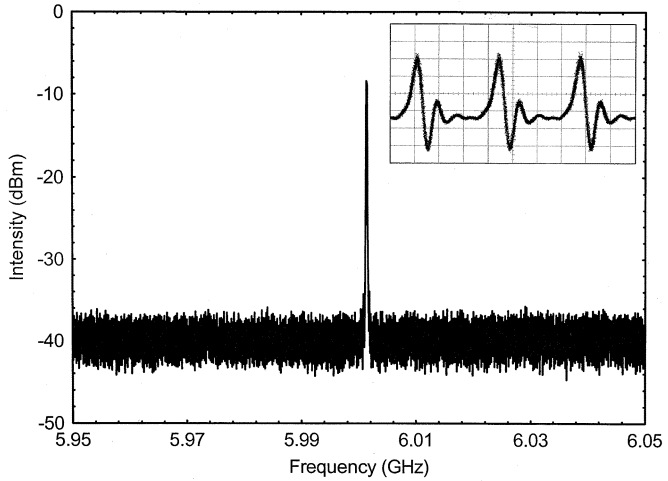

Fig. 8. RF spectrum and sampling oscilloscope trace (inset) of the output pulse with 25-m DCF in the cavity.

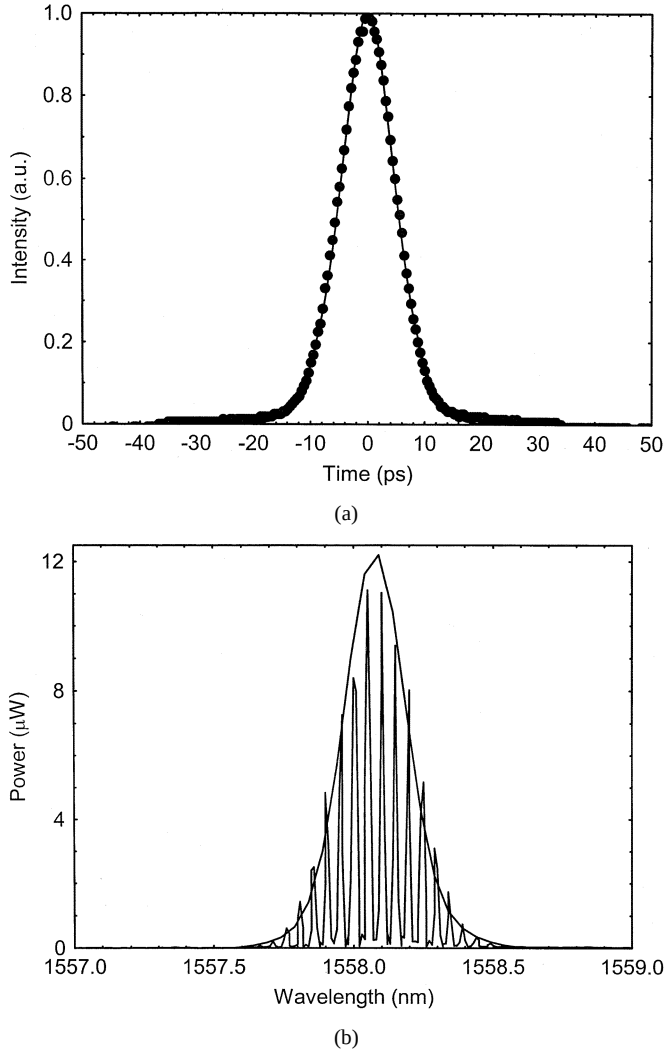

Fig. 9. Pulse characteristics in time and frequency domains when the intracavity dispersion is normal. (a) Autocorrelation trace (points are experimental results and the curves is from the numerical model). (b) Spectrum (the envelope curve is numerical result).

characteristics (pulsewidth, spectral width, and time-bandwidth product) are found stable over the entire tuning span, as shown in Fig. 11. Pulsewidth ranges from 11.4 to 11.9 ps and time-bandwidth product ranges between 0.35 and 0.45.

B. Simulation

The same numerical model has been run with the experimental parameters in normal dispersion regime. The settings of the system are similar to those in the anomalous-dispersion case

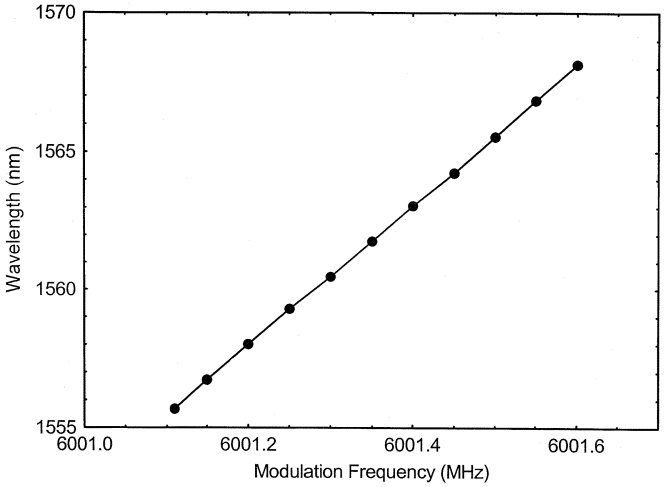

Fig. 10. Oscillating wavelength versus modulation frequency in normal dispersion regime (25-m DCF inserted in the cavity).

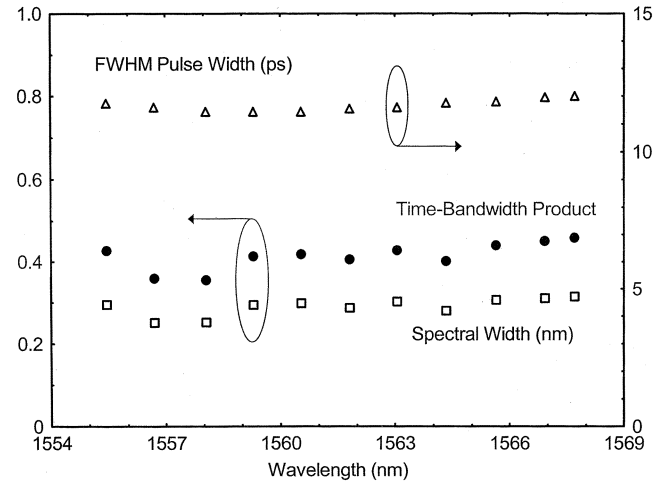

Fig. 11. Pulse characteristics versus oscillating wavelength during dispersion tuning with 25-m DCF in the cavity.

except that the 100m-SMF-28 is replaced by 25-m DCF with a dispersion parameter of -88 ps/(km · nm). Fig. 12 shows the formation of stable solutions in time and frequency domains from an arbitrarily defined seed pulse. The calculated temporal and spectral widths are 11.4 ps and 0.25 nm, which again agree well with the experiment. The time dependence of the pulse intensity and the frequency chirp are plotted in Fig. 13. In clear contrast to the anomalous-dispersion case shown in Fig. 7, the chirp is flat and close to zero across the entire pulse, indicating near-TL pulses. The autocorrelation functions and the spectrum from the model agree well with the experimental results, as shown in Fig. 9.

IV. Discussion

There are two key elements in our design of smoothly wavelength-tunable HMLFRLs—the dispersion and the SOA. Each element has two distinct operating states. The dispersion can be either anomalous or normal. The SOA can be dc biased (a modulator is necessary to actively mode-lock the laser) or ac modulated (no modulator is needed as the SOA itself is the mode-locking element). The combination of the two elements leads to four possible system configurations. In our previous paper [10], we analyzed the combination of anomalous dispersion and a dc-operated SOA. In Sections II and III, the two cases with the SOA in ac operation were discussed. Our simulation and preliminary experiment showed that the combination of normal dispersion and a dc-operated SOA produced strongly blue-chirped pulses and hence required a few kilometers of SMF-28 fiber for pulse compression, which is highly undesirable for practical pulse generators. Therefore, this configuration is excluded from the following comparisons. The performances of the other three configurations are summarized in Table I.

Two comparisons can be made from Table I. The first and the second columns of the table show the comparison between the dc and the ac operations of the SOA in the anomalous dispersion regime. In both configurations, pulse compression is necessary to obtain picosecond pulses. However, with the same amount of intracavity dispersion (100 m of SMF-28 in both cases), directly modulating the SOA produces shorter pulses, even at a lower repetition frequency. Two factors may contribute to this difference. First, direct gain modulation produces stronger frequency chirp and hence greater spectral broadening. This is evident by comparing the spectral widths of the two cases. Second, the linearity of the chirp also influences the pulsewidth after the compression. Root-mean-square (rms) time-bandwidth product has to be used to characterize the output pulses when the SOA is dc operated due to the large deviation of the pulse shape from Sech^2 [10]. The value is much larger than the TL-limited values of some regular pulse shapes such as Gaussian and Sech^2, indicating that the pulses can not be well compressed by linear pulse compression. This is likely due to the strong nonlinear chirp caused by the SOA. On the other hand, the ac operated SOA leads to near-linear chirp and a time-bandwidth product much closer to the transform-limited value of Sech^2 distribution. The direct modulation of the SOA also results in a slightly broader tuning range and much smaller polarization sensitivity. The latter is due to the elimination of the polarization-sensitive EO modulator. At last, the dc operation of the SOA provides better SMN suppression than the ac operation of the SOA. This is likely due to the lower bias (smaller gain) of the SOA in the ac operation case [10].

The second and the third columns of Table I show the other comparison, which is between the normal and the anomalous dispersion regimes when the SOA is in ac operation. Both configurations are polarization insensitive and have similar SMN suppression ratio, while the tuning range is slightly wider and the time-bandwidth product is slightly smaller in the normal regime. No pulse compression is required to obtain near-TL pulses in the normal regime, which is the most significant improvement over the anomalous regime. As a tradeoff, however, the output pulses from a normal-dispersion cavity are much broader.

Overall, the ac operation of the SOA outperforms the dc operation of the SOA in most aspects, with simpler structure, smaller polarization sensitivity, wider tuning range, more regular pulse shape and the option of shorter pulses or the elimination of the pulse compression. Depending on the requirements on pulse width and pulse compression in particular applications, one can

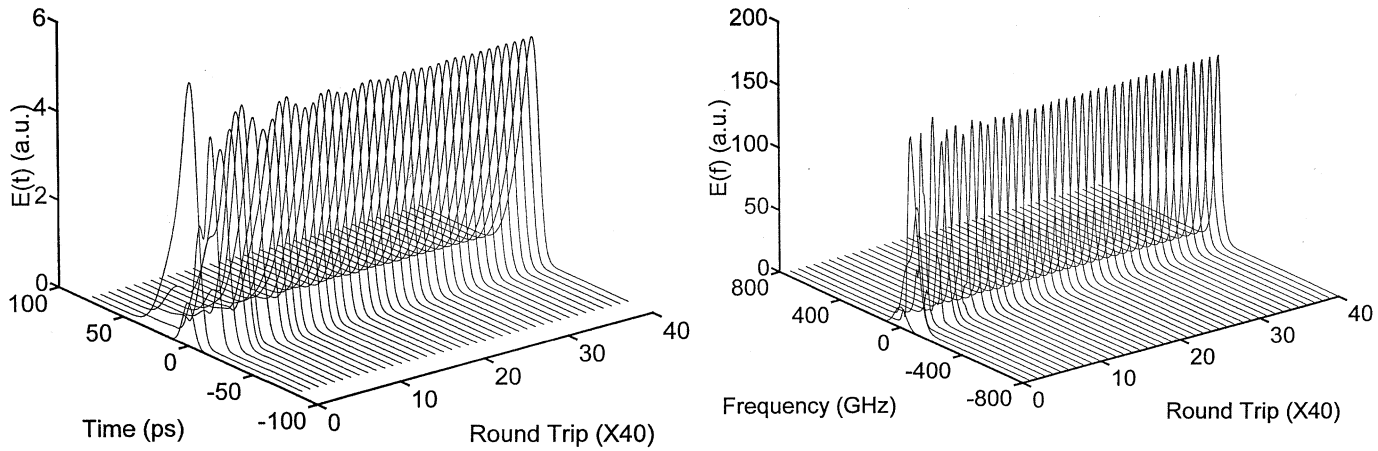

Fig. 12. Stable solutions establish from an initial pulse in both time (left) and spectral (right) domains after 1600 round-trips.

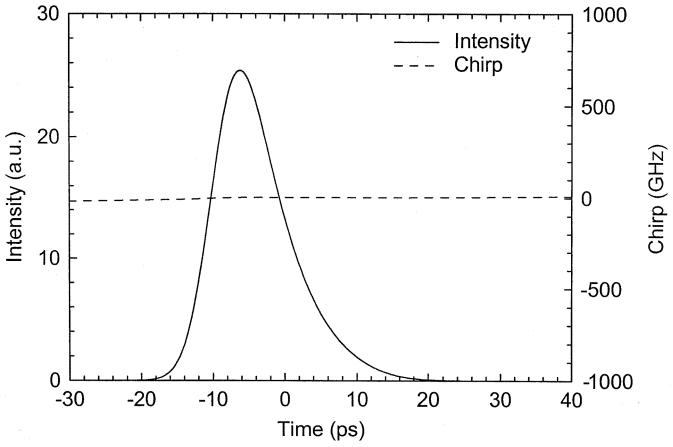

Fig. 13. Time dependence of the intensity and the frequency chirp of the simulated output pulses when the intracavity dispersion is normal.

TABLE I
PERFORMANCE COMPARISON OF THREE DIFFERENT CONFIGURATIONS

	DC & Anomalous (100 m SMF-28)	AC & Anomalous (100 m SMF-28)	AC & Normal (25 m DCF)
Δt (FWHM)	5.3 ps (10 GHz)	3.7 ps (6 GHz)	11.4 ps (6 GHz)
Δλ (3 dB)	0.27 nm	0.94 nm	0.25 nm
Δt·Δf	0.95 (RMS)	0.43	0.35
Compression	Yes	Yes	No
Tuning Range	10 nm	11 nm	12 nm
Polarization Sensitivity	Large	Small	Small
SMN Suppression Ratio	33 dB	28 dB	29 dB

choose normal or anomalous dispersion to combine with the directly modulated SOA. The SMN suppression ratio can be improved by increasing the bias current of the SOA. But more efficient RF coupling is required to ensure a sufficiently large modulation depth.

The tuning range is determined by two factors—the gain profile against wavelength and the total intracavity dispersion. As pointed out by Zhao *et al.* [7], the CW modes always compete with the mode-locked modes in a dispersion-tuned HMLFRL due to the absence of spectral filtering and the homogeneous nature of the gain medium. When the locked modes are tuned to the edge of the gain band, the CW modes near the gain peak may acquire sufficient power to quench the locked modes. Therefore, a wide and flat gain profile is ideal for broadening the tuning range. In our case, the gain profile of the system is a combination of the gain profiles of the EDFA and the SOA. Varying the pumping of either amplifier results in a different overall gain profile. This explains the slightly different tuning ranges in the three cases in Table I. In fact, a much broader tuning range (∼20 nm) was observed when a different SOA (E-TEK) was used in our experiment.

The amount of dispersion inside the cavity may also have impact on the tuning range. This is easy to understand when considering the basic mode-locking condition

$$T_{rt} = \frac{L}{v_g(\lambda)} \tag{1}$$

where T_{rt} is the round-trip time of the pulses; L is the length of the cavity and $v_g(\lambda)$ is the group velocity of the pulses, which is a function of wavelength in a dispersive cavity. The round-trip time is related to the modulation frequency by the equation of $T_{rt} \equiv m/f_m$, where f_m is the pulse repetition frequency and m is the harmonic order. For a fixed value of f_m, (1) has a series of solutions of λ corresponding to different values of m. The two adjacent solutions are separated by a wavelength spacing of

$$\Delta\lambda = \frac{1}{DLf_m} \tag{2}$$

where D is the dispersion parameter of the fiber and defined as $D = d(1/v_g)/d\lambda$. (2) shows that the spacing between two neighboring synchronization wavelengths is inverse proportional to the total dispersion of the fiber loop, DL, when the modulation frequency is fixed. When DL is sufficiently large, $\Delta\lambda$ may become smaller than the gain band and lead to dual-wavelength operation [6]. The competition between the two wavelengths may further limit the tuning range. Therefore,

the tuning range is determined by the gain profile of the system when $\Delta\lambda$ is larger than the gain band and by both gain profile and total dispersion when $\Delta\lambda$ is smaller than the gain band. A brief estimation using (2) shows that, for all the three cases in Table I, $\Delta\lambda$ is approximately 50 nm, which is much greater than the measured tuning range. Thus the tuning range is gain-band limited in these cases. Dual-wavelength operation has been observed in our experiment when 100-m DCF is used in the cavity. This agrees with above analysis considering that $\Delta\lambda$ becomes about 12 nm in this case, which is about the same as the gain-band limited tuning range.

Another important issue is long-term stability, which has become a major challenge in building practical HMLFRLs [1]. There are two mechanisms causing instability—cavity length drift and polarization fluctuation, both stemming from the long fiber cavities of HMLFRLs [1]. With dispersion tuning, however, any drift in cavity length due to environmental changes (temperature, vibration, etc.) is automatically transformed to wavelength variation while the laser stays mode-locked [6]. Moreover, by replacing the EO modulator with a directly modulated, polarization-insensitive SOA, the effect of polarization fluctuation is minimized. Therefore, a dispersion-tuned HMLFRL with a directly modulated SOA is robust to external perturbations and hence has good long-term stability. Stable pulsing over a few hours has been observed in our experiment. It should be pointed out that wavelength stability is traded off for pulsing stability in dispersion-tuned systems. To stabilize wavelength, ambient control or a length-frequency compensation system may be needed.

V. Conclusion

We have experimentally and numerically demonstrated a simple design of a stable, smoothly wavelength-tunable picosecond optical pulse generator, in which a dispersive fiber ring laser is actively mode-locked by modulating an SOA. The essence of this idea is to properly combine the effects of the fast gain saturation and saturation induced SPM of the SOA and the intracavity dispersion to produce linearly chirped or chirp-free pulses while utilizing dispersion tuning to achieve smooth wavelength tuning. The SOA also effectively suppresses the supermode noise and reduces the polarization sensitivity of the laser. Much improved performances have been achieved over previously reported systems. Comparisons also reveal the different characteristics of the laser in normal and anomalous dispersion regimes. The numerical simulation shows good agreement with the experiment and hence confirms the operation principle of the system. The tuning range is determined by both the gain profile and the total intracavity dispersion. Dispersion tuning and the low polarization sensitivity of the SOA ensure the long-term stability of the system.

This work opens the possibility of using dispersion and SOAs to construct practical tunable pecosecond pulse sources. An interesting scheme is to build a wavelength-scanable pulse generator, which is able to produce a stable pulse train whose color is continuously sweeping within a certain wavelength range. This kind of systems can be easily realized from our experimental setup by electrically controlling the modulation frequency or the cavity length and should be able to find many applications in photonic testing.

Acknowledgment

The authors would like to thank Dr. C. J. K. Richardson for his valuable comments.

References

[1] S. Kawanishi, "Ultrahigh-speed optical time-division-multiplexed transmission technology based on optical signal processing," *IEEE J. Quantum Electron.*, vol. 34, pp. 2064–2079, 1998.

[2] R. P. Davey, K. Smith, and A. McGuire, "High-speed, mode-locked, tunable, integrated erbium fiber laser," *Electron. Lett.*, vol. 28, pp. 482–483, 1992.

[3] H. Takara, S. Kawanishi, and M. Saruwatari, "20 GHz transform-limited optical pulse generation and bit-error-free operation using a tunable, actively modelocked Er-doped fiber ring laser," *Electron. Lett.*, vol. 29, pp. 1149–1150, 1993.

[4] D. H. Kim, S. H. Kim, Y. M. Jhon, Y. T. Byun, J. C. Jo, and S. S. Choi, "Ultrahigh-speed fiber-integrated semiconductor ring laser," *Opt. Commun.*, vol. 181, pp. 385–390, 2000.

[5] T. Pfeiffer and G. Veith, "40 GHz pulse generation using a widely tunable all-polarization preserving erbium fiber ring laser," *Electron. Lett.*, vol. 29, pp. 1849–1850, 1993.

[6] S. Li and K. T. Chan, "Electrical wavelength tunable and multiwavelength actively mode-locked fiber ring laser," *Appl. Phys. Lett.*, vol. 72, pp. 1954–1956, 1998.

[7] Y. Zhao, C. Shu, J. H. Chen, and F. S. Choa, "Wavelength tuning of 1/2-rational harmonically mode-locked pulses in a cavity-dispersive fiber laser," *Appl. Phys. Lett.*, vol. 73, pp. 3483–3485, 1998.

[8] A. D. Ellis, R. J. Manning, I. D. Phillips, and D. Nesset, "1.6 ps pulse generation at 40 GHz in phaselocked ring laser incorporating highly nonlinear fiber for application to 160 Gbit/s OTDM networks," *Electron. Lett.*, vol. 35, pp. 645–646, 1999.

[9] J. S. Wey, J. Goldhar, and G. L. Burdge, "Active harmonic modelocking of an erbium fiber laser with intracavity Fabry–Pérot filters," *J. Lightwave Technol.*, vol. 15, pp. 1171–1180, July 1997.

[10] L. Duan, C. J. K. Richardson, Z. Hu, M. Dagenais, and J. Goldhar, "A stable smoothly wavelength-tunable picosecond pulse generator," *IEEE Photon. Technol. Lett.*, vol. 14, pp. 840–842, June 2002.

[11] R. S. Tucker, S. K. Korotky, G. Eisenstein, U. Koren, L. W. Stulz, and J. J. Veselka, "20 GHz active mode-locking of a 1.55 μm InGaAsP laser," *Electron. Lett.*, vol. 21, pp. 239–240, 1985.

[12] S. W. Corzine, J. E. Bowers, G. Przybylek, U. Koren, B. I. Miller, and C. E. Soccolich, "Actively mode-locked GaInAsP laser with subpicosecond output," *Appl. Phys. Lett.*, vol. 52, pp. 348–350, 1988.

[13] D. J. Kuizenga and A. E. Siegman, "FM and AM mode locking of the homogeneous laser—Part I: Theory," *IEEE J. Quantum Electron.*, vol. QE-6, pp. 694–708, 1970.

[14] G. P. Agrawal and N. K. Dutta, *Semiconductor Lasers*, 2nd ed: Van Nortrand Reinhold, 1993, ch. 11.

[15] K. L. Hall, G. Lenz, A. M. Darwish, and E. P. Ippen, "Subpicosecond gain and index nonlinearities in InGaAsP diode lasers," *Opt. Commun.*, vol. 111, pp. 589–612, 1994.

Lingze Duan (M'02) was born in Beijing, China, in 1971. He received the B.S. degree in physics from Tsinghua University, Beijing, in 1995 and the M.S. and Ph. D degrees in electrical engineering from the University of Maryland, College Park, in 1998 and 2002, respectively.

He is currently a Postdoctoral Associate at the Research Laboratory of Electronics (RLE), Massachusetts Institute of Technology (MIT), Cambridge. His research has been focusing on mode-locking optical pulse generation and ultrashort pulse characterization.

Dr. Duan is a Member of the IEEE Lasers and Electro-Optics Society (LEOS) and of the Optical Society of America (OSA).

Mario Dagenais (SM'02) received the B.S. degree from the Université de Montréal, QC, Canada, in 1974 and the M.S. and Ph.D. degrees from the University of Rochester, Rochester, NY, in 1976 and 1978, respectively.

From 1978 to 1980, he joined Prof. N. Bloembergen at Harvard University as a Research Fellow. After working at the GTE corporate research laboratory, Waltham, MA, for six years, he joined the faculty of the University of Maryland, College Park, in 1987 as an Associate Professor and was named Professor of Electrical Engineering in 1992. From 1994 to 2000, he served as Director of the National Science Foundation's Center for Optoelectronic Devices, Interconnects, and Packaging (COEDIP) at the University of Maryland, a leading University/Industry Center. In 1998, he cofounded Quantum Photonics, a prominent semiconductor laser and semiconductor laser amplifier supplier for the fiber optics industry. He originally served as Quantum Photonics' President and CEO and then as Chief Technology Officer. In January 2003, he returned to his previous position at the University of Maryland and he is currently Director of the Photonic Switching and Integrated Optoelectronic Laboratory. He is also a Professor of Electrical and Computer Engineering at the University of Maryland. He has more than 26 years of experience in the area of optoelectronics. His expertise includes high-power semiconductor lasers, semiconductor optical amplifiers, and integrated optoelectronics. He has coedited the book *Integrated Optoelectronics* and has authored or coauthored more than 200 technical publications. He has provided consulting services to a number of industry leaders.

Dr. Dagenais has organized several national and international conferences.

Julius Goldhar, photograph and biography not available at the time of publication.